

# Experimental and Theoretical Research on Welded Aluminum K-Joints <sup>†</sup>

Šemso Kalač <sup>1,\*</sup>, Martin Mensinger <sup>2</sup>, Christina Radlbeck <sup>2</sup>, Naja Zejnelagić <sup>3</sup>, Đorđe Đuričić <sup>4</sup> and Duško Lučić <sup>3</sup>

<sup>1</sup> Faculty of Polytechnics, University Donja Gorica, 81000 Podgorica, Montenegro

<sup>2</sup> School of Engineering and Design, Technical University of Munich, 80333 Munich, Germany; mensinger@tum.de (M.M.); c.radlbeck@tum.de (C.R.)

<sup>3</sup> Civil Engineering Faculty, University of Montenegro, 81000 Podgorica, Montenegro; zejnelagicnaja\_94@hotmail.com (N.Z.); dlucic@ucg.ac.me (D.L.)

<sup>4</sup> College of Applied Sciences Uzice, 31000 Uzice, Serbia; djordje.djuric@vpts.edu.rs

\* Correspondence: semso.kalac@udg.edu.me; Tel.: +382-69-218-525

<sup>†</sup> Presented at the 15th International Aluminium Conference, Québec, QC, Canada, 11–13 October 2023.

**Abstract:** Aluminum alloys provide corrosion resistance, lightweight construction, and functionality through extruded profiles. The creation of heat-affected zones (HAZs), which can reduce load-bearing capacity by up to 50% and complicate K-joint design, makes it difficult to apply aluminum in truss systems. Since EN 1999-1-1 (EC 9) does not even provide guidelines for welded aluminum K-joints, practitioners turn to EN 1993-1-8 (EC 3), resulting in a conservative design that ignores the advantages of aluminum. This study investigated the behavior of welded K-joints in lattice girders made of alloy EN AW 6082 T6. The comparison of the experimental and numerical results showed different load-bearing behaviors depending on dimensions and cross-section types. Further tests were carried out. The aim was to derive an aluminum-specific design procedure.

**Keywords:** aluminum alloys; welded joints; K-joint; HAZ; Eurocode; experiment; lattice girder; Eksteoris Var



**Citation:** Kalač, Š.; Mensinger, M.; Radlbeck, C.; Zejnelagić, N.; Đuričić, Đ.; Lučić, D. Experimental and Theoretical Research on Welded Aluminum K-Joints. *Eng. Proc.* **2023**, *43*, 18. <https://doi.org/10.3390/engproc2023043018>

Academic Editor: Mario Fafard

Published: 13 September 2023



**Copyright:** © 2023 by the authors. Licensee MDPI, Basel, Switzerland. This article is an open access article distributed under the terms and conditions of the Creative Commons Attribution (CC BY) license (<https://creativecommons.org/licenses/by/4.0/>).

## 1. Introduction

Aluminum alloys reach tensile strengths of up to 500 MPa through the alloying process, which is comparable to high-strength steel and provides high corrosion resistance. At the same time, remelting and recycling aluminum and its alloys is a cost-effective and simple process that makes this metal an ecologically and economically viable building material. Because of its formability, it is easy to cast or extrude complex shapes.

Lattice girders made of hollow sections (HSS—hollow section structure), which can be circular (CHS—circular hollow section), square (SHS—square hollow section), or rectangular (RHS—rectangular hollow section), have several advantages over lattice girders made of hot-rolled open sections, such as easy assembly, high load-bearing capacity, a low aerodynamic coefficient, and the use of internal space.

The combination of the high load-bearing capacity and low aerodynamic coefficient of HSS lattice girders with the low weight, high corrosion resistance, and high tensile strength of aluminum alloys could lead to competitive aluminum structures with large spans. This is especially true for areas with aggressive environmental conditions where high-quality maintenance cannot be guaranteed.

However, in order to achieve this, it is necessary to take into account the peculiarities that occur in aluminum alloys due to welding and the particular type of joint defects in HSS lattice girders.

Welding causes weakening zones, known as heat-affected zones (HAZs), in many aluminum alloys, which reduce the load-bearing capacity of the structure by up to 50%.

On the other hand, the design of connections within a lattice structure is critical to the rationality and feasibility of a given structure. The quality of the designed connections affects not only the cost of the structure, but also the speed of assembly, the possibility of reuse, and the guarantee of quality and safety. Direct welding of the brace to the chord members is the simplest method of connecting the members of a lattice structure made of HSS sections. Compared with indirect welding, direct welding provides greater structural integrity and technical safety. Forces between the elements are transmitted directly.

With the exception of Al alloys in the annealed and T4 condition, EN 1999 [1,2] does not specifically address the calculation of K-joints in aluminum structures but relies on the calculation of welds according to EN 1993-1-8 [3], the standard for steel structures. Accordingly, appropriate reduction factors are applied. This approach is conservative and negates the positive effects of aluminum alloys as a material for welded HSS lattice girders.

The task set by the “Eksteoris Var” project, which this research is a part of, is to define clear expressions or approaches on how to rationally calculate the load capacity of aluminum HSS welded joints as part of lattice girders to make structures with large spans competitive and rational.

## 2. Previous Research

Previous research in this area can be divided into two categories. The first group includes HAZ research on the mechanical properties of aluminum alloys. The second category includes studies on the load-bearing capacity of lattice girder joints. With the exception of Đorđe Đuričić [4], whose research deals with the load-bearing capacity of K-joints made from a CHS profile of aluminum alloy EN AW 6082-T6, research in the second group has predominantly been performed on steel trusses.

The following conclusions were derived by Y.F.W. Lai and D.A. Nethercot (1993) [5] after studying the load-bearing capacity of aluminum elements with local transverse welds. Even though a HAZ's dimensions are small, it is not safe to ignore its softening effect on columns that are welded at the ends. When the HAZ is in the middle of the column, the load-bearing capacity of the column is reduced the most. The column then behaves exactly as if it were completely in the HAZ.

R. Deekhunthod (2014) [6] investigated the quality of aluminum alloy welds in his dissertation. The paper included analyses from a variety of fields. Some final conclusions were drawn from the results and observations. There was no discernible difference in tensile strength or yield strength between welded samples from different ingots. MIG welding had an impact on the microstructure and mechanical properties of the HAZ. The HAZ extends 20 mm from the fusion line for a plate thickness of 5 mm.

R. Feng and B. Young (2011) [7] used finite element analysis to investigate cold-formed tubular T- and X-joints with a compressed chord member. Y. Chen, R. Feng, and X. Ruan (2016) [8] presented experimental testing and finite element analysis of X-joints with double square hollow sections (SHSs) under axial pressure, which were reinforced with concrete in the zone between the inner and outer tubes, in their paper “Behaviour of steel-concrete-steel SHS X-joints under Axial Compression”. Y. Chen, R. Feng, and L. Fu (2017) [9] investigated the effects of axial pressure on empty and filled square hollow section (SHS) stainless steel X- and T-nodes. A total of 24 samples were evaluated, including empty tubular joints and tubular joints.

Djuricic Dj (2018) [4] studied K-joints created using CHS aluminum profiles experimentally, theoretically, and numerically. The research goal was to establish analytical expressions that allow the use of formulae from EN 1993 parts 1-8 for the computation of K- and T-joints in the nodes of aluminum lattice constructions. This was accomplished by incorporating a new softening coefficient and modifying the expressions proposed in the steel structure standard. A numerical analysis of K-joints constructed from CHS aluminum profiles was performed by Kalac S, Zejnelagic N, Djuricic Dj, and Lucic D. (2022) [10].

### 3. Theoretical Background and Materials

Directly welded joints for structural components are classified according to their shape, such as planar X-, T-, Y-, N-, and K-joints, as well as special KT-, DK-, and DY-joints, and spatial XX-, TT-, and KK-joints [3]. The distribution of forces inside the joint determines the configuration of a welded joint, which includes the joint form, gap (+g), overlap (=−g), eccentricity (e), and angle of inclination of the brace member [11]. Figure 1 shows examples of K-, Y-, and X-joint types that illustrate the aforementioned properties.

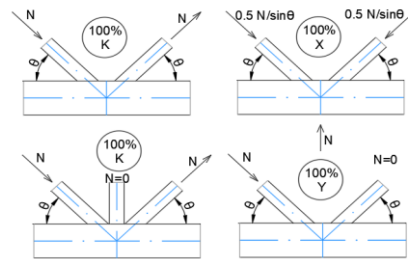


**Figure 1.** Configuration of directly welded joints.

Following the transfer of load inside a joint, potential fracture locations and thus potential fracture forms can be determined, where the stiffness distribution in combination with the material characteristics of the given location determine the fracture form. The lowest load at which a fracture occurs at one of the possible points defines the load-bearing capacity of the connection.

This study addresses a specific failure mode, the plastification of the chord face, which occurs as the main failure mode when the ratio between the width of the brace and the width of the chord member is less than 0.85. Several criteria can be used to characterize a section's load-bearing capacity, but the limit state of deformations is the most generally utilized criterion for joints. To limit the amplitude of deformations, the limit state of local deflection of the chord member face in proximity to the welded brace member, defined by the chord member width ( $b_o$ ), has been proposed by Lu et al. [12]. For square (SHS) and rectangular (RHS) hollow section profiles, most rules specify a maximum local deflection of  $3\% b_o$ , as shown in Figure 2. Furthermore, in the serviceability limit state, an arbitration value of  $1\% b_o$  is adopted for RHS and SHS profiles.

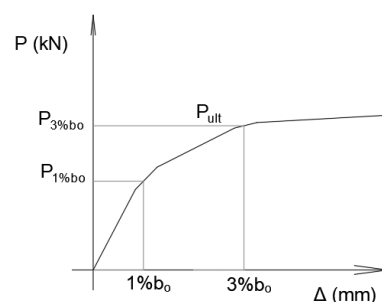


**Figure 2.** Deformation limit criteria.

The most commonly used aluminum alloy for structures is EN AW 6082 T6, which has the yield strength of steel S235. As a result of material softening during the welding process, this alloy is known to have a reduction in yield stress of up to 50% within the heat-affected zone (HAZ); therefore, this alloy was selected for this study.

Magnesium (Mg) and silicon (Si) are the most common alloying elements and are dominant in this alloy. Magnesium influences the melting point at  $541\text{ }^{\circ}\text{C}$  as well as the increase in load capacity and resistance to corrosion caused by salt water. Silicon also influences the melting point reduction as well as strength and ductility [13].

The 6xxx alloy series belongs to a group of aluminum alloys that are subject to thermo-mechanical treatment. These alloys show the best mechanical and physical properties

when they are artificially aged, which includes solution annealing, tempering, and aging at defined temperatures for a certain time. This process has a direct influence on the physical and mechanical properties of the alloy after the heat treatment [14].

The reduction coefficient  $\rho_{o,HAZ}$ , defined in EN 1999-1-1 [1,2], accounts for the reduction in yield stress that occurs within the heat-affected zones (HAZs) of welded aluminum joints. When employing this coefficient, the entire joint is assumed to be within the HAZ. However, as described in Table 1, EN 1999 part 1-1 also gives explicit recommendations for identifying the borders of the HAZ depending on its width ( $b_{HAZ}$ ).

**Table 1.**  $b_{HAZ}$  values depending on element thickness and welding method [1].

The Thickness of the Member $t$ (mm)	MIG $b_{HAZ}$ (mm)	TIG $b_{HAZ}$ (mm)
$0 < t \leq 6$	20	30
$6 < t \leq 12$	30	30 (to 35)
$12 < t \leq 25$	35	35 (to 40)
$t > 25$	40	40 (to 50)

#### 4. Experimental Investigations

Six lattice girders manufactured from the aluminum alloy EN AW6082 T6 in total were investigated in this experiment. Brace members and chord members were joined together directly using TIG welding with the filler rod ER 5356 (AlMg5).

The lattice girders had a height of 600 mm and a 3000 mm span. All tested lattice girders had the same chord members, which were SHS 100 × 5 profiles. In order to carry out the parametric analysis, the brace members' shape and size were altered. Circular hollow sections (CHSs) with cross-sectional diameters of 40, 50, and 60 mm were used to construct three lattice girders. Brace members from SHS profiles with widths of 40, 50, and 60 mm were used to construct the other three lattice girders. According to the profiles of the cross-sections of the brace members, the lattice girders received their names. Lattice girders with square brace profiles were labeled SHS40, SHS50, and SHS60 as a result. On the other hand, lattice girders with circular hollow section profiles for brace members were identified as CHS40, CHS50, and CHS60. Regarding this, the  $\beta$  coefficient varied from 0.4 (SHS40 and CHS40) to 0.6 (SHS60 and CHS 60), which refers to the ratio of the width or diameter of the brace member to the width of the chord member. The joints met all the requirements of EN 1993-1-8 [3] and were both concentric and with a gap.

The lattice girders were simply supported at points A and B, installed in an indeterminate frame (C), and loaded with a concentrated single force (D) in the middle of the span. Local Y-joint deformation above supports was avoided (A and B). In order to prevent backing, the lattice girders' compressed chord members were laterally supported every 500 mm with bolts in a point connected with U steel profiles (E). The compression force transducer (I), which stood on a steel plate with dimensions 120 × 30 × 100, received the force from the hydraulic press (D) above.

The local deflection of chord members' faces was measured using displacement transducers that were fixed to them. As shown in Figures 3 and 4, displacement transducers attached to chord members (III, IV, and V) measured local deflections for K-joints, while displacement transducers attached to the steel frame (VI and VII) measured the global deflection of the lattice girders. Meanwhile, the displacement transducer II measured the X-joint's local displacement.

The forces inside brace and chord members were calculated indirectly using the known relationship between axial force and normal stress and the relationship between normal stress and strain because the stresses were lower than the proportionality limit of the  $\sigma$ - $\epsilon$  curve on which Hooke's law can be applied. Strains were measured using strain gauges installed at the center of the faces of members, as shown in Figures 3 and 4. Strain gauges 1–4 were related to the compressed chord member, strain gauges 5–8 to the tensioned chord member, strain gauges 9–12 to the compressed brace member in the middle

of the span, strain gauges 13–16 to the tensioned brace member, and strain gauges 17–20 to the compressed brace member at the end of lattice girder, as shown at Figure 3.

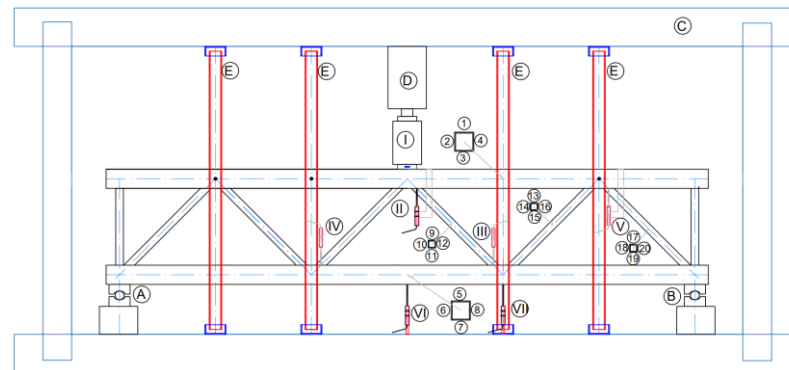


**Figure 3.** Schematic disposition of aluminum lattice girder testing.



**Figure 4.** Disposition of aluminum lattice girder testing.

Figure 4 demonstrates the investigation of two K-joints in the tensioned chord member (KTL and KTR) and one K-joint in the compressed chord member (KC). The local deflection was measured using displacement transducer III for the KTR joint and transducers IV and V for the KTL and KC joints, respectively. The forces inside the compressed braces were obtained indirectly via strain gauges positioned in the middle of each side of the brace, whereas the forces inside the chord members were measured indirectly via strain gauges in the same manner.

## 5. Results

### 5.1. Experimental Results

The leading critical load was determined for all six lattice girders studied via the chord area plastification of the X-joint, then the KC-joint, and finally the KTL- and KTR-joints. Experimental results for the load-bearing capacity of K-joint face plastification in SHS 60 and CHS 60 samples were not obtained due to the full plastification of the X-joint in the observed lattice girder. The diagrams below were produced. The following diagrams, such as the one shown in Figure 5, were prepared based on the results of the test.

As shown in Figure 5, there was a good match between the load-bearing capacity results for K-joints of the same lattice girder. Because of its low utilization of the chord members' cross-section load-bearing capacity, the influence of axial force inside the chord members on the load-bearing capacity of the K-joints could be neglected. In the following chart (Figure 6), force–deflection curves for the K-joints of all investigated lattice girders are presented.

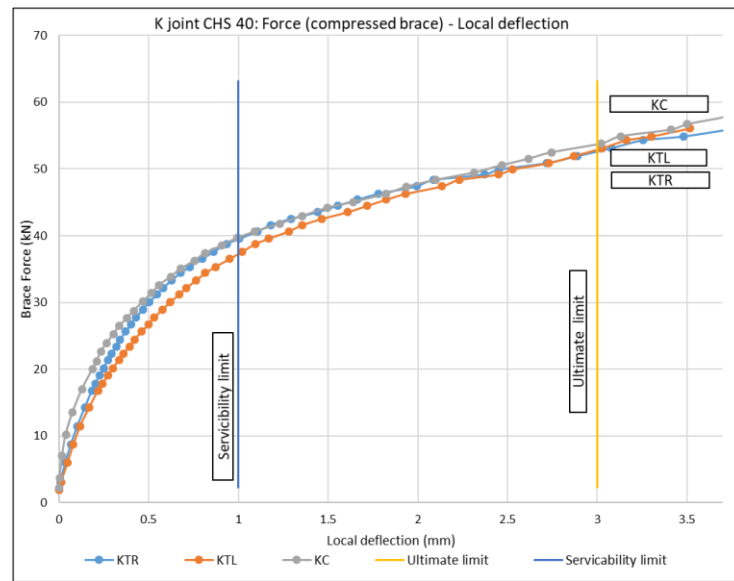


Figure 5. Force–deflection curves for K-joints of CHS 40 lattice girder.

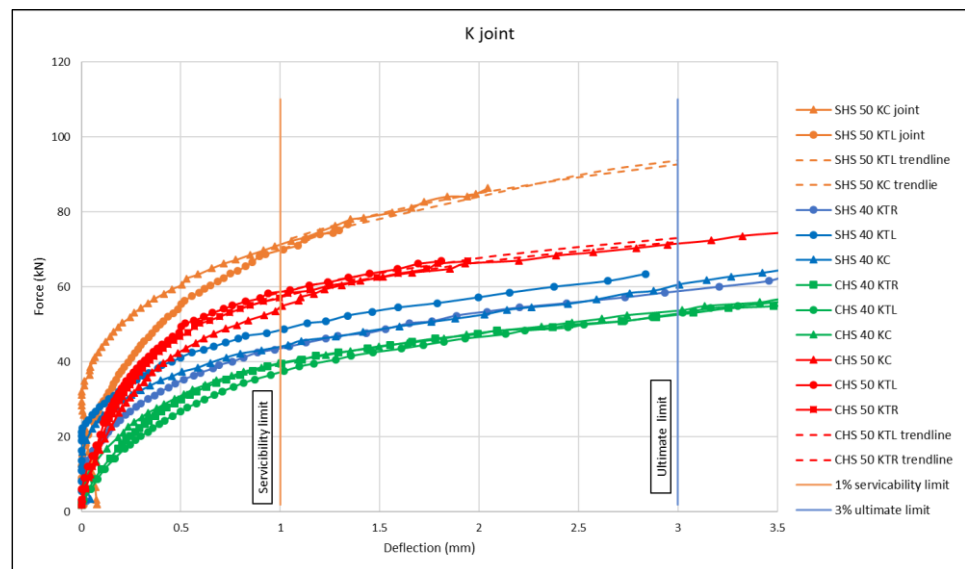


Figure 6. Force–deflection curves for K-joints.

The results of the load-bearing capacities of the K-joints are shown in Table 2.  $P_{1\%bo}$  represents the force inside the brace member at the serviceability limit, and  $P_{ult,exp}$  represents the force at the joint’s ultimate limit or load-bearing capacity.

Figure 7 shows samples of deformed K-joints after they have reached load-bearing capacity. The left sides of the samples show plastification of the chord face under the axially compressed brace member, whose deflection was measured as a deformation limit criterium, whereas the right sides show plastification of the chord face due to the tensioned brace member. This represents typical K-joint axially loaded deformation for the chord face plastification failure mode. The left sample includes CHS brace members, and the right sample includes SHS brace members.

**Table 2.** The load-bearing capacities of K-joints experimental results.

Specimen	K-Joint	$\beta$	$P_{1\%b_0}$ (kN)	$P_{ult,exp}$ (kN)
SHS 40	KTR	0.4	43.6	58.8
SHS 40	KTL	0.4	48.5	64.6
SHS 40	KC	0.4	44.1	60.6
SHS 50	KTR	0.5	N/A	N/A
SHS 50	KTL	0.5	70.0	93.7
SHS 50	KC	0.5	71.3	92.7
CHS 40	KTR	0.4	39.5	52.6
CHS 40	KTL	0.4	37.3	52.9
CHS 40	KC	0.4	39.7	53.7
CHS 50	KTR	0.5	57.9	71.9
CHS 50	KTL	0.5	58.8	73.1
CHS 50	KC	0.5	54.7	71.5

**Figure 7.** K-joint face plastification failure.

### 5.2. Theoretical Results according to EN 1993 and EN 1999

In EN 1993-1-8 [3] the design axial resistance for welded steel K-joints is defined with the following expression (1):

$$N_{1,Rd} = \frac{8.9 \cdot \gamma^{0.5} \cdot k_n \cdot f_{y0} \cdot t_0^2}{\sin \theta_i} \left( \frac{b_1 + b_2}{b_0} \right) / \gamma_{M5} \quad (1)$$

$k_n$ —coefficient that takes into consideration the forces inside the chord member;

$f_{y0}$ —the yield strength of the chord member;

$\theta_i$ —the included angle between the brace member and the chord;

$t_0$ —the wall thickness of the chord member;

$\gamma_{M5}$ —partial safety factors for hollow section joints, in this case, taken as 1.0;

$b_0, b_1,$  and  $b_2$ —widths of chord and brace members.

For the values for the case in which we have CHS brace members instead of SHS brace members, expression (1) has to be multiplied by  $\Pi/4$ . The values for the ultimate limit state of K-joints without considering the influence in the HAZ according to EN 1993-1-8 [2] are given in Table 3.

**Table 3.** Characteristic values of forces inside brace members for K-joints according to EN 1993-1-8 [2] and EN 1999 part 1-1.

Specimen	K-Joint	$\beta$	$P_{ult,EN1993}$ (kN)	$P_{ult,EN1993+EN1999}$ (kN)
SHS 40	KTR, KTL, and KC	0.4	111.2	55.6
SHS 50	KTR, KTL, and KC	0.5	139.0	69.5
CHS 40	KTR, KTL, and KC	0.4	87.3	43.7
CHS 50	KTR, KTL, and KC	0.5	109.1	54.8

On the other hand, the reduction coefficient  $\rho_{0,HAZ}$  is introduced in EN 1999-1-1 [1,2], which considers the reduction in yield strength in the HAZ. When expression (1) is multiplied by the reduction coefficient  $\rho_{0,HAZ}$ , the load-bearing capacity of the K-joint inside the brace member is given using expression (2):

$$N_{1,Rd} = \rho_{0,HAZ} \cdot \frac{8.9 \cdot \gamma^{0.5} \cdot k_n \cdot f_{y0} \cdot t_0^2}{\sin \theta_i} \left( \frac{b_1 + b_2}{b_0} \right) / \gamma_{M5} \quad (2)$$

According to EN 1999-1-1 [1,2], the value of  $\rho_{0,HAZ} = 0.5$  for aluminum alloy EN AW6082 T6. The values of the load-bearing capacities of the K-joints according to expression (2) are given in Table 3, which considers the reduction in yield strength in the HAZ.

## 6. Discussion

Experimentally obtained values of the load-bearing capacities of the K-joints were generally lower than values obtained using expression (1), based on EN 1993-1-8, but they were higher than values obtained using expression (2), based on EN 1993-1-8 and EN 1999-1-1, especially for higher values of the  $\beta$  coefficient. The experimental results of the K-joints, particularly with SHS brace members, show that the values obtained with expression (1) are quite conservative and do not reflect the true behaviors of these joints. Table 4 summarizes the results of the load-bearing capacities of the K-joints based on the experimental outputs, EN 1993-1-8 and EN 1993-1-8 + EN 1999-1-1.

**Table 4.** The load-bearing capacities of K-joints.

Specimen	K-Joint	$\beta$	$P_{ult,EN1993+EN1999}$ (kN)	$P_{ult,exp}$ (kN)	$P_{ult,EN1993}$ (kN)
SHS 40	KTR	0.4	55.6	58.8	111.2
SHS 40	KTL	0.4	55.6	64.6	111.2
SHS 40	KC	0.4	55.6	60.6	111.2
SHS 50	KTR	0.5	69.5	N/A	139.0
SHS 50	KTL	0.5	69.5	93.7	139.0
SHS 50	KC	0.5	69.5	92.7	139.0
CHS 40	KTR	0.4	43.7	52.6	87.3
CHS 40	KTL	0.4	43.7	52.9	87.3
CHS 40	KC	0.4	43.7	53.7	87.3
CHS 50	KTR	0.5	54.8	71.9	109.1
CHS 50	KTL	0.5	54.8	73.1	109.1
CHS 50	KC	0.5	54.8	71.5	109.1

## 7. Conclusions

The design of welded connections in aluminum lattice girders is an interesting topic in civil engineering. The current design standard for aluminum structures, EN 1999-1-1 [1,2], does not contain specific provisions for the calculation of welded HSS connections. Therefore, the rules in EN 1993-1-8 [3], a standard primarily intended for the design of steel connections, currently serve as a guide for the design of equivalent welded connections in aluminum structures.

The leading critical load was determined in this study using six lattice girders by plasticizing the K-joint chord surface. However, the experimentally determined values of the load-bearing capacities of the K-joints were, as expected, significantly lower than the values obtained using expression (1) based on EN 1993-1-8 for steel without a HAZ. On the other hand, the experimentally determined values were greater than the values determined using expression (2) based on EN 1993-1-8 and EN 1999-1-1. This was observed especially for higher values of the  $\beta$  coefficient. Further experiments are planned. The aim is to derive an aluminum-specific design procedure.

**Author Contributions:** Conceptualization, Š.K. and C.R.; methodology, Š.K. and D.L.; experimental investigation, Š.K., N.Z. and Đ.Đ.; validation, D.L., C.R. and M.M.; formal analysis, Š.K.; resources, Š.K.; writing—original draft preparation, Š.K.; writing—review and editing, C.R.; visualization, Š.K.; supervision, C.R., D.L. and M.M.; project administration, Š.K. All authors have read and agreed to the published version of the manuscript.

**Funding:** This research received no external funding.

**Informed Consent Statement:** Not applicable.

**Data Availability Statement:** The data presented in this study are available on request from the corresponding author. The data are not publicly available due to privacy and confidentiality concerns.

**Conflicts of Interest:** The authors declare no conflict of interest. The funders had no role in the design of this study; in the collection, analysis, or interpretation of the data; in the writing of the manuscript; or in the decision to publish the results.

## References

1. European Committee for Standardization. *prEN 1999-1-1: Design of Aluminium Structures—Part 1-1: General Structural Rules*; European Committee for Standardization: Brussels, Belgium, 2020.
2. European Committee for Standardization. *EN 1999-1-1:2019, Eurocode 9: Design of Aluminium Structures—Part 1-1*; European Committee for Standardization: Brussels, Belgium, 2007. Available online: <https://www.phd.eng.br/wp-content/uploads/2014/11/en.1999.1.1.2007.pdf> (accessed on 1 September 2023).
3. European Committee for Standardization. *Eurocode 3: Design of Steel Structures—Part 1-8: Design of Joints*; European Committee for Standardization: Brussels, Belgium, 2005. Available online: <https://www.phd.eng.br/wp-content/uploads/2015/12/en.1993.1.8.2005-1.pdf> (accessed on 1 September 2023).
4. Đuričić, Đ. Experimental and Theoretical Analysis of Limit States of Aluminum Lattice Structures. Doctoral Thesis, University of Montenegro, Podgorica, Montenegro, 2018.
5. Lai, Y.F.W.; Nethercot, D.A. Strength of aluminium members containing local transverse welds. *Constr. Build. Mater.* **1993**, *7*, 27–39. [[CrossRef](#)]
6. Deekhunthod, R. Weld Quality in Aluminium Alloys. Ph.D. Dissertation, Uppsala University, Uppsala, Sweden, 2014.
7. Feng, R.; Young, B. Design of cold-formed stainless-steel tubular T- and X-joints. *J. Constr. Steel Res.* **2011**, *67*, 421–436. [[CrossRef](#)]
8. Chen, Y.; Feng, R.; Ruan, X. Behaviour of steel-concrete-steel SHS X-joints under Axial Compression. *J. Constr. Steel Res.* **2016**, *122*, 469–487. [[CrossRef](#)]
9. Chen, Y.; Feng, R.; Fu, L. Investigation of grouted stainless steel SHS tubular X- and T-joints subjected to axial compression. *Eng. Struct.* **2017**, *150*, 318–333. [[CrossRef](#)]
10. Kalac, S.; Zejnelagic, N.; Djuricic, D.; Lucic, D. Proposal of an analytical expression for determination of load capacity for aluminum square hollow section (SHS) K-joint under chord tension. In Proceedings of the 8th International Conference “Civil Engineering-Science and Practice”, Kolašin, Montenegro, 8–12 March 2022.
11. Wardenier, J.; Packer, J.; Zhao, X.; van der Vegte, G. *Hollow Sections in Structural Applications*, 3rd ed.; CIDECT: Geneva, Switzerland, 2002.
12. Lu, L.H.; De Winkel, G.D.; Yu, Y.; Wardenier, J. Deformation limit for the ultimate strength of hollow section joints. In Proceedings of the Sixth International Symposium on Tubular Structures, Melbourne, Australia, 14–16 December 1994.
13. Mazzolani, F. *Aluminium Alloy Structures*, 2nd ed.; E & FN Spon: London, UK, 1994.
14. Stamenkovic, U.; Ivanov, S.; Markovic, I.; Strbac, N.; Mitovski, A. The influence of the temperature of solution heat treatment on the properties of 6000 series aluminium alloys. *Tehnika* **2017**, *72*, 523–527. [[CrossRef](#)]

**Disclaimer/Publisher’s Note:** The statements, opinions and data contained in all publications are solely those of the individual author(s) and contributor(s) and not of MDPI and/or the editor(s). MDPI and/or the editor(s) disclaim responsibility for any injury to people or property resulting from any ideas, methods, instructions or products referred to in the content.